Hindawi
Wireless Communications and Mobile Computing
Volume 2022, Article ID 9041184, 12 pages
https://doi.org/10.1155/2022/9041184

Research Article

An Intelligent Hough Transform with Jaya of Multipopulation Cooperation for Diameter Estimation of Red-Hot Workpiece

Xinyu Zhang[1,2] **Ke Chen**[1,2] **Rong Mu**[1,2] **Yanxi Yang**[1,2] **and Jinghua Li**[1,2]

[1]*Shaanxi Key Laboratory of Complex System Control and Intelligent Information Processing, Xi'an University of Technology, Xi'an 710048, China*
[2]*Faculty of Automation and Information Engineering, Xi'an University of Technology, Xi'an 710048, China*

Correspondence should be addressed to Xinyu Zhang; xhyzzxy@126.com

Received 4 February 2022; Accepted 23 March 2022; Published 8 April 2022

Academic Editor: Mingqian Liu

Diameter is a critical metric during producing circular workpieces, but it is always challenging to measure accurately due to the existence of noise. The intelligent Hough transform with Jaya (IHTJ) is developed to solve this issue recently. However, it suffers from some disadvantages including unsatisfactory accuracy and convergence rate caused by the problem of trapping into local optimization in the case of inaccurate priori knowledge. In this paper, an IHTJ of multipopulation cooperation (IHTJMC) is proposed to overcome these disadvantages. Firstly, we analyse the problem of IHTJ in the diameter measurement. Secondly, a ring structure of the multipopulation cooperation is designed. In this structure, the whole population is divided into several subpopulations which evolve independently all the time. This can ensure a few best and worst solutions guide the evolution of the whole population at the same time. Then, we propose a migration strategy to finish the cooperation among the different subpopulations, which selects a few individuals from each subpopulation randomly, and exchange them with each other. This strategy can make the different subpopulations share the information among the entire population and improve the global search ability. Finally, three experiments are introduced to test the effectiveness of the IHTJMC. The experimental results demonstrate that the IHTJMC can restrain the problem of falling into local optimization significantly. Compared with the existing methods, it has superior accuracy and robustness for the diameter measurement of a circular workpiece which is heated to red state.

1. Introduction

Diameter is a critical parameter in many fields including monitoring the state of trains, inspecting the fuel injection, ceramic cylindrical workpiece manufacturing, polymeric fibre production, and monocrystal silicon growth [1–5]. In these fields, the diameter can be used to evaluate the quality of products or the operation state of equipment. If the diameter cannot be measured accurately, some unqualified products or faults cannot be found in time. This will lead to large economic losses or disasters. As a result, it is vital to measure the diameters precisely for some crucial workpiece production. However, it is very difficult to measure the diameter with the traditional contact measuring technologies in some high-temperature environments. For example, the traditional contact measuring technologies for the diameter have great limitations when the workpieces are burned red in the production of hot forgings. With the rapid development of charge coupled device (CCD) sensor and digital image processing technology, the diameter measurement based on the image processing technology has been developed [6–8]. Because this method is noncontact and has a high precision, it is used to measure the circular workpiece's diameter which is red-hot. The process of diameter measurement based on the image processing technology is as follows: firstly, capture the image of the circular workpiece by a CCD camera, and the workpiece is elliptical in the image because of the shooting angle; secondly, segment the image and extract the edge of the workpiece; finally, apply an ellipse fitting method to fit these extracted edge points, so as to obtain the diameter of the workpiece [9]. However, there are some heat radiation and dust in the production of hot forgings, which results

in massive noise in the previous image processing. This makes the edge points not be completely located on an ideal ellipse. As a result, it is really hard to get the precise parameters of the ellipse which consists of the edge points, and the diameter measurement cannot be obtained precisely. Consequently, it is so crucial to present a strong estimation method for elliptical parameters to measure diameter when the edge points of a red-hot circular workpiece include much noise.

Recently, lots of ellipse fitting methods have been proposed. They are mainly divided into three categories. The first category is the least square (LS) method. This kind of method searches the optimal ellipse parameters through making the distance between the ideal and real ellipse minimum. Its strengths are good realizability and instantaneity, but its robustness is unsatisfactory due to the effect of the noise, so its precision and robustness are poor [6, 10–12]. The second category is random sample consistency (RANSAC). In RANSAC, a subset is sampled from the edge points and then tested whether the points outside the subset meet the model. If so, the points are put into subsets. Repeat the above steps and get the subset including the most edge points so as to obtain the optimal ellipse which is corresponding to this subset. Compared with the LS method, RANSAC is more robust, but its detection accuracy is limited by the iterative times. When the iterative time is unreasonable, the errors of ellipse parameters are very large [13–15]. The last category is Hough transform (HT). This method maps the ellipse model into the parameter space and searches the optimal ellipse parameters by the enumeration in this space. Compared with the previous two categories, the HT method has stronger robustness and higher accuracy, so it is widely used in elliptic fitting [16–18]. However, the HT has some terrible disadvantages, such as the bad real-time performance and high memory footprint. As a result, it is very difficult to implement in the real application [19–21]. To overcome these, many scholars have developed the improved methods. Xu et al. propose the random HT (RHT) in [22], which greatly reduces memory consumption and computation by sampling pixels randomly. However, its performance is obviously impacted by noise in the image because of the introduction of solving equations. And then, a circle HT (CHT) architecture is proposed in [23], which can reduce the memory by 74% to 93%, with little reduction inaccuracy. It is utilized to find the inner and outer iris boundaries in eye images, but the accuracy and real-time performance of this method may decrease when there is additive Gaussian noise in the images. In [24], to solve the problem of low real-time performance in the track-before-detect algorithm based on HT (HT-TBD), an adaptive real-time recursive radial distance-time plane HT-TBD method was proposed. This method takes advantage of the adaptive approach to adjust the parameter space to realize the recursive detection. It can effectively raise the real-time performance of the method. With the development of artificial intelligence (AI) methods, some AI methods have been introduced in signal processing [25–27]. Recently, Zhang et al. propose an intelligent HT with Jaya (IHTJ) in [28], which transforms the ellipse fitting into an optimal problem, thus using Jaya to seek the optimum solution in the parameter space. The speed and accuracy of the HT are improved greatly. However, although Jaya has the good global search ability, it is unavoidable to trap into local optimization, and the convergence rate of the method gets slow when the range of the initial values is set unreasonable. This is because the prior knowledge cannot be obtained precisely in most practical applications, especially there are lots of noise in the edge points during the process of measuring the diameter of the red-hot circular workpiece. Therefore, it is really critical for the IHTJ to improve its global search ability so as to increase the accuracy and speed of measuring the diameter of the circular workpiece which is heated to red.

In this paper, an IHTJ of multipopulation cooperation (IHTJMC) is developed to overcome the issue in the diameter measurement of a circular workpiece which is heated to the red-hot state. The major work of this paper are as follows:

(1) We describe the problem of the diameter measurement in the production of a circular workpiece and analyse the reasons for the disadvantages of IHTJ

(2) An intelligent ring structure of multipopulation cooperation is proposed. It can improve the global search ability through dividing the population into several subpopulations which evolves independently with their own best and worst solutions

(3) We design the cooperative strategy based on the migration between the different subpopulations. This can enhance the global search ability and convergence rate further through exchanging the information among different subpopulations, so as to increase the accuracy and robustness of the diameter measurement

(4) The proposed method is tested by simulation and practical experiments, and the results are satisfactory

The remainder of this paper is summarized as follows: Section 2 introduces the problem of diameter measurement in the production of the red-hot circular workpiece and describes the disadvantages of the IHTJ. And the detail of the proposed method is introduced in Section 3. Section 4 makes the verification for the performance of the proposed method according to the simulation and practical experiments. Section 5 presents the conclusion.

2. Problem Description and IHTJ Review

2.1. Problem Description. In the process of producing a red-hot circular workpiece, it is really hard to measure its diameter directly due to the high-temperature environment. A noncontact measuring method is adopted to overcome this issue, which introduces the CCD and digital image processing technology. Figure 1 is the schematic of its principle. As shown in this figure, a CCD camera is installed above the workpiece to collect its image, and then, the edge point set

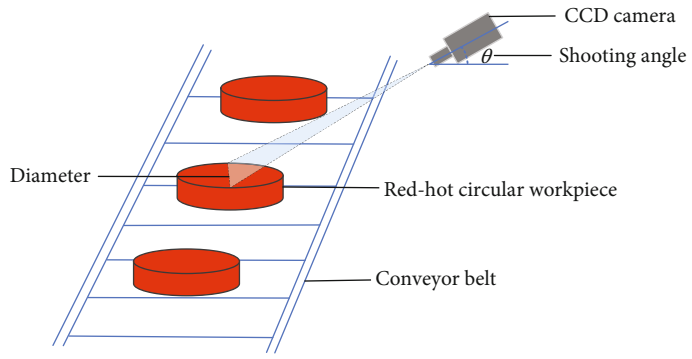

Figure 1: Principle of diameter measurement for red-hot workpieces with CCD camera.

of the workpiece contour can be obtained by image segmentation and edge extraction. Because there is an angle between the camera and the surface of the workpiece, the real diameter in the vertical direction shortens in the image and the contour of the circle workpiece is an ellipse in the image (the effect of errors and deviations is not considered here). Hence, the workpiece's diameter will be estimated by fitting these edge points.

Assume that the point set obtained through the edge extraction is $I = \{(x_1, y_1), (x_2, y_2), \cdots, (x_n, y_n)\}$, where n is the number of points in the set. Elliptic equation can be described as follows [9].

$$\frac{(x - x_c)^2}{a^2} + \frac{(y - y_c)^2}{b^2} = 1, \tag{1}$$

where a is the semimajor axis of the ellipse, b is the semiminor axis of the ellipse, and (x_c, y_c) is the centre coordinate of the ellipse.

Through fitting (1) with the set of edge points, the parameters of ellipse (a, b, x_c, y_c) can be obtained, and thus, the diameter of circular workpiece $2a$ can be obtained. Therefore, the diameter measurement is transformed into the ellipse fitting according to the point set. And the performance of diameter measurement depends on the ellipse fitting method [9].

2.2. IHTJ Review. HT is widely used to fit the ellipse because of its strong robustness, but it is not easy to realize in many practical problems. This is because it uses the exhaustive method, which leads to the bad real-time performance and high memory occupation. Especially, it gets worse in ellipse fitting because there are four parameters in an elliptic equation at least. To address this issue, the IHTJ is proposed in [28]. This method maps (1) into the parameter space and designs a fitness function firstly, and then, it transforms the ellipse fitting to seek the optimum value in the parametric space, which can get the peak value of the HT's accumulator. The fitness function is expressed by

$$F(a, b, x_c, y_c) = \sum_{i=1}^{n} f(a, b, x_c, y_c, x_i, y_i), \tag{2}$$

$$f(a, b, x_c, y_c, x_i, y_i) = \begin{cases} 0, & \psi(a, b, x_c, y_c, x_i, y_i) > T_f, \\ 1, & \psi(a, b, x_c, y_c, x_i, y_i) \le T_f, \end{cases} \tag{3}$$

$$\psi(a, b, x_c, y_c, x_i, y_i) = \left| \frac{(x_i - x_c)^2}{a^2} + \frac{(y_i - y_c)^2}{b^2} - 1 \right|, \tag{4}$$

where $F(a, b, x_c, y_c)$ is the accumulator of (a, b, x_c, y_c) in the HT method. Since it is impossible that all of the points are on the ellipse due to the existence of noise, a threshold T_f is considered in this equation, which can enhance the robustness of the method.

Then, an intelligent optimization method known as Jaya is introduced to overcome this problem and the IHTJ is developed. This method decreases the computational complexity and memory occupation of the HT greatly without any loss of robustness and accuracy. However, although Jaya has excellent global search ability, it still suffers from the problem of falling into local optimum. In some practical applications, it is very hard to obtain the prior information about the circular workpiece, so the scope of initial values cannot be set very accurate. This makes the problem of falling into local optimum worsen significantly, and it results in unsatisfactory convergence rate and diameter measurement of the red-hot workpiece. Therefore, it is really critical to improve the accuracy and convergence rate of IHTJ in the case of inaccurate scope of initial values during measuring the circular workpiece's diameter when it is heated red.

3. Proposed Method

To solve the problem that the IHTJ method falls into local optimal solution easily when the scope of initial values is inaccurate, this paper proposes an IHTJMC method that designs the structure of multipopulation cooperation and the collaborative strategy between different populations, so as to strengthen the information exchange and global search ability. Compared with the IHTJ method, this method can improve the convergence rate and the accuracy of diameter measurement due to the use of multipopulation cooperation. Meanwhile, it maintains the great robustness of the HT. In the following subsections, the details of IHTJMC and the full procedure are described.

3.1. Structure of Multipopulation Cooperation in IHTJMC. Due to the advantages of the small number of parameters and simple realization, Jaya is introduced into the IHTJ method to find the optimal solution in the parametric space for the diameter measurement of the red-hot circular workpiece. Unlike other swarm intelligence algorithms and evolutionary algorithms, Jaya considers the impacts of the optimal and the worst solution at the same time, so it has advanced optimization accuracy and search efficiency [29, 30]. And the IHTJ method has better efficiency and speed compared with the general HT. However, the similarity of the populations continues to increase with the increasing iterations, and the diversity of the whole population is low. As a result, the Jaya and IHTJ method are easy to trap in the local optimization, which misleads the results.

To improve the global search ability of the IHTJ, a collaborative structure of multipopulation is proposed in this paper. It is shown as Figure 2. In this structure, the whole population is divided into M subpopulations randomly after the initialization. The number of individuals in each subpopulation is N. At the beginning of every iteration, the cooperation is implemented between different subpopulations through the designed migration strategy. A few individuals are, respectively, chosen from subpopulation j and subpopulation $j+1$ randomly, where $j = 1, \cdots, M\text{-}1$, and then exchange them with each other. Next, do this operation in turn until $j = M - 1$. When $j = M$, sample the individuals from subpopulation M and subpopulation 1 randomly and replace them with each other. After that, all subpopulations form a ring structure, and the cooperation is finished in each subpopulation with the migration between the two different subpopulations. This structure introduces the idea of cooperation and improves the population diversities to improve the global search capability of Jaya by exchanging information between different subpopulations. Then, each subpopulation keeps independent all the time, and they finish the generation of new individuals through the mechanism of Jaya, in which the own best and worst individuals of each subpopulation are used to update the individuals. The details will be introduced in Section 3.2. At last, the global optimal solution is obtained from these M subpopulations.

Compared with the IHTJ, the proposed method introduces the multipopulation cooperation structure. It finishes the population evolution by dividing the whole population into M subpopulations rather than only one population. In this process, each subpopulation updates its individuals based on its own best and worst individual. This can enhance the diversity of population through implementing the population evolution based on more than one best and worst individual. Meanwhile, the cooperations between different subpopulations are achieved by the migration. It can improve the global search ability further by sharing the information between different subpopulations. Hence, it is helpful for the IHTJMC to raise the convergence rate of the method and the measuring accuracy of the red-hot workpiece's diameter, especially when the scope of initial values is inaccurate.

3.2. Optimization Strategy of IHTJMC. In the IHTJMC of this paper, the multipopulation migration is designed to realize the cooperation between different subpopulations. The purpose is to improve the population diversity through dispersing the entire population into a few subpopulations and sharing the information between different subpopulations. In this strategy, each subpopulation can search its own global optimal solution in its own subregion independently. Then, some individuals are sampled randomly from one subpopulation and are migrated into another. At the same time, the same number of individuals is also selected from the other subpopulation at random and migrated into this one. The historical and present information can be shared among different subpopulations effectively. Compared with the evolution including only one population, it is beneficial to improve the diversity of the entire population and the global search ability when some best and worst individuals guide the evolution of the population at the same time. As a result, IHTJMC can restrain the problem of local optimization while maintaining the superiority of IHTJ.

3.2.1. Fitness Function of IHTJMC. To maintain the superiority of the HT, the fitness function has been designed in the IHTJ method. This fitness function converts the ellipse fitting into the optimal problem of seeking the best elliptical parameters in the parametric space after the HT. It retains the robustness and precision of the HT as well as improving its real-time performance and memory occupancy through the introduction of the intelligent optimization algorithms. In order to guarantee that the algorithm has the great robustness, this fitness function is reserved in the IHTJMC. It is shown as (2)–(4) in Section 2.2.

3.2.2. Population Initialization. During the initialization, some parameters are set. They include the size of the population NP, the number of subpopulation M, the number of iterations G, and the initial population $\mathbf{x}_l = [x_1, x_2, x_3, x_4]$, where $l = 1, 2, \cdots, NP$. In $\mathbf{x}_l$, the four components are defined by the elliptical parameters. They are as follows: $x_1 = a$, $x_2 = b$, $x_3 = x_c$, and $x_4 = y_c$. In order to make the initial population cover the entire search space very well, the chaotic mapping is used to generate the initial individuals. It is calculated by

$$\mathbf{x}_l = \mathbf{x}^{\mathrm{L}} + \left(\mathbf{x}^{\mathrm{U}} - \mathbf{x}^{\mathrm{L}}\right) \times \tilde{\mathbf{x}}_l, \tag{5}$$

$$\tilde{\mathbf{x}}_l = \mu \cdot \tilde{\mathbf{x}}_{l-1}\left(1 - \tilde{\mathbf{x}}_{l-1}\right), \tag{6}$$

where $\mathbf{x}_l$ represents the $l_{\text{-th}}$ individual in the initial population, $\mathbf{x}^{\mathrm{U}}$ is the upper boundary, $\mathbf{x}^{\mathrm{L}}$ is the lower boundary, μ is the chaos factor and it is set to 4 in general, and $\tilde{\mathbf{x}}_l$ is the $l_{\text{-th}}$ individual after the chaotic mapping.

3.2.3. Subpopulation Division. To implement the multipopulation cooperation, NP individuals are divided into M subpopulations randomly after the population initialization, and the number of the individuals in each subpopulation N is NP/M. Throughout the process of iteration, these M subpopulations are always kept separated. Every

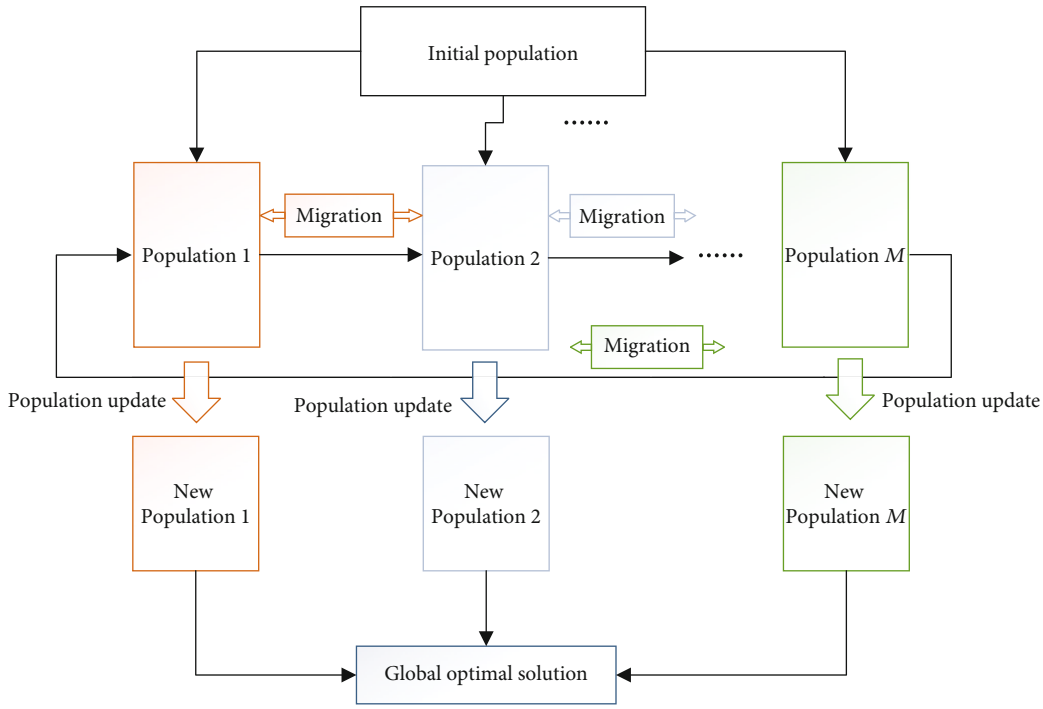

Figure 2: Collaborative structure of multipopulation.

subpopulation possesses its best and worst individual, and these best and worst individuals direct the evolution of its own subpopulation.

3.2.4. Subpopulation Migration. In the IHTJMC, migration is an important part which is used to achieve the cooperation between the different subpopulations. It can ensure that the information is shared among the different subpopulations. Based on the ring structure designed in Section 3.1, choose 20% of the individuals from the $j_{\text{-th}}$ and $(j+1)_{\text{-th}}$ subpopulation at random, respectively. Then, exchange these individuals between each other's subpopulations. Repeat this operation until $j = M - 1$. When $j = M$, do that between the $M_{\text{-th}}$ and first subpopulation. After that, all of subpopulations have finished the migration, and the cooperation of them has been achieved through the ring structure. As a result, the information from different subpopulations will enhance the search capacity of each subpopulation. It lays a good foundation for the generation of new individuals and the evolution of the whole population.

3.2.5. New Individual Generation. After the migration of subpopulations, these M subpopulations begin to iterate and evolve independently. Each subpopulation generates new individuals in its own search space. The new individual generation is expressed by

$$\mathbf{x}'^{k}_{l,j} = \mathbf{x}^{k}_{l,j} + \mathbf{r}_1\left(\mathbf{x}^{k}_{\text{best},j} - \left|\mathbf{x}^{k}_{l,j}\right|\right) - \mathbf{r}_2\left(\mathbf{x}^{k}_{\text{worst},j} - \left|\mathbf{x}^{k}_{l,j}\right|\right), \quad (7)$$

where $\mathbf{x}'^{k}_{l,j}$ represents the $l_{\text{-th}}$ new individual of the $j_{\text{-th}}$ population in the $k_{\text{-th}}$ iteration, $l = 1, \cdots, N$, $\mathbf{r}_1$, and $\mathbf{r}_2$ are the vectors sampled from [0,1] randomly, and $\mathbf{x}^{k}_{\text{best},j}$ and $\mathbf{x}^{k}_{\text{worst},j}$ represent the best and worst individual of the $j_{\text{-th}}$ population in the $k_{\text{-th}}$ iteration, respectively. The idea of "seeking advantages and avoiding disadvantages" is well reflected in (7). $\mathbf{r}_1(\mathbf{x}^{k}_{\text{best},j} - |\mathbf{x}^{k}_{l,j}|)$ corresponds to "advantages-seeking," which shows that the individuals of each subpopulation get close to the present optimal individual in the process of iteration constantly; $-\mathbf{r}_2(\mathbf{x}^{k}_{\text{worst},j} - |\mathbf{x}^{k}_{l,j}|)$ corresponds to "disadvantages-avoiding," which expresses that the individuals in each population keep moving away from the present worst individual in the iterative process.

3.2.6. Illegal Individuals Treatment. After generating new individuals, each subpopulation needs to detect whether the newly generated individuals are within the normal range. If not, these individuals are called illegal individuals and need to be repaired. They are repaired by

$$x'^{k}_{m,l,j} = \begin{cases} 2x^{\text{U}}_{m} - x'^{k}_{m,l,j}, & x'^{k}_{m,l,j} > x^{\text{U}}_{m}, \\ 2x^{\text{L}}_{m} - x'^{k}_{m,l,j}, & x'^{k}_{m,l,j} < x^{\text{L}}_{m}, \\ x'^{k}_{m,l,j}, & \text{otherwise}, \end{cases} \quad (8)$$

where $x'^{k}_{m,l,j}$ represents the $m_{\text{-th}}$ component of $\mathbf{x}'^{k}_{l,j}$, $m = 1, \cdots, 4$, and x^{U}_{m} and x^{L}_{m} are the upper and lower boundary of the $m_{\text{-th}}$ component, respectively.

3.2.7. Population Update. In this paper, the purpose is to search the maximum value of the fitness function in the parameter space after transforming the ellipse fitting into the optimization problem. As a result, it is necessary to

compare the fitness function value of the new individual $\mathbf{x}'^{k}_{l,j}$ with that of the previous individual $\mathbf{x}^{k}_{l,j}$ and determine which of them should be preserved into the $(k+1)_{\text{-th}}$ iteration. The individual update is calculated by

$$\mathbf{x}^{k+1}_{l,j} = \begin{cases} \mathbf{x}^{k}_{l,j} & F\left(\mathbf{x}'^{k}_{l,j}\right) \le F\left(\mathbf{x}^{k}_{l,j}\right), \\ \mathbf{x}'^{k}_{l,j} & F\left(\mathbf{x}'^{k}_{l,j}\right) > F\left(\mathbf{x}^{k}_{l,j}\right), \end{cases} \tag{9}$$

where $F(\cdot)$ represents the fitness function value which is determined by (2)-(4) in Section 2.2. As can be seen from (9), the new individual which owns lager fitness function value than the previous will be saved for the next iteration. Otherwise, it will be discarded and the previous one will be preserved into the next iteration. This can make the algorithm obtain the optimal solution in each subpopulation after a few iterations.

3.2.8. Best and Worst Individual Renewal. When all of the individuals in the M subpopulations are renewed, the best individual and the worst individual of every subpopulation in the $(k+1)_{\text{-th}}$ iteration are updated as follows:

$$\begin{cases} \mathbf{x}^{k+1}_{\text{best},j} = \arg\max\limits_{\mathbf{x}^{k+1}_{l,j}} F\left(\mathbf{x}^{k+1}_{l,j}\right), \\ \mathbf{x}^{k+1}_{\text{worst},j} = \arg\min\limits_{\mathbf{x}^{k+1}_{l,j}} F\left(\mathbf{x}^{k+1}_{l,j}\right). \end{cases} \tag{10}$$

At the same time, the best individual $\mathbf{x}^{k+1}_{\text{best}}$ and the worst individual $\mathbf{x}^{k+1}_{\text{worst}}$ of the whole population must be updated, too. They are obtained by

$$\begin{cases} \mathbf{x}^{k+1}_{\text{best}} = \arg\max\limits_{\mathbf{x}^{k+1}_{\text{best},j}} F\left(\mathbf{x}^{k+1}_{\text{best},j}\right), \\ \mathbf{x}^{k+1}_{\text{worst}} = \arg\min\limits_{\mathbf{x}^{k+1}_{\text{worst},j}} F\left(\mathbf{x}^{k+1}_{\text{worst},j}\right). \end{cases} \tag{11}$$

In the IHTJMC method, the processes of subpopulation migration, new individual generation, illegal individual treatment, population update, and best and worst individual renewal are implemented in turn repeatedly until it reaches the maximum number of iterations or stopping condition. Then, the optimal solution $\mathbf{x}_{\text{best}}$ is obtained in the last iteration, which makes the fitness function maximum. And the optimal parameters of the ellipse can be obtained, thereby obtaining the optimal measurement of the red-hot workpiece's diameter.

Compared with the HT, the IHTJMC can increase the running speed and decrease the memory occupation significantly because it uses the Jaya with multipopulation cooperation rather than traverses all of the solutions in the parametric space. Compared with the IHTJ, the IHTJMC increases the measuring accuracy and restrains the problem of trapping into the local optimization through introducing the optimization strategy based on the cooperation of the multipopulation.

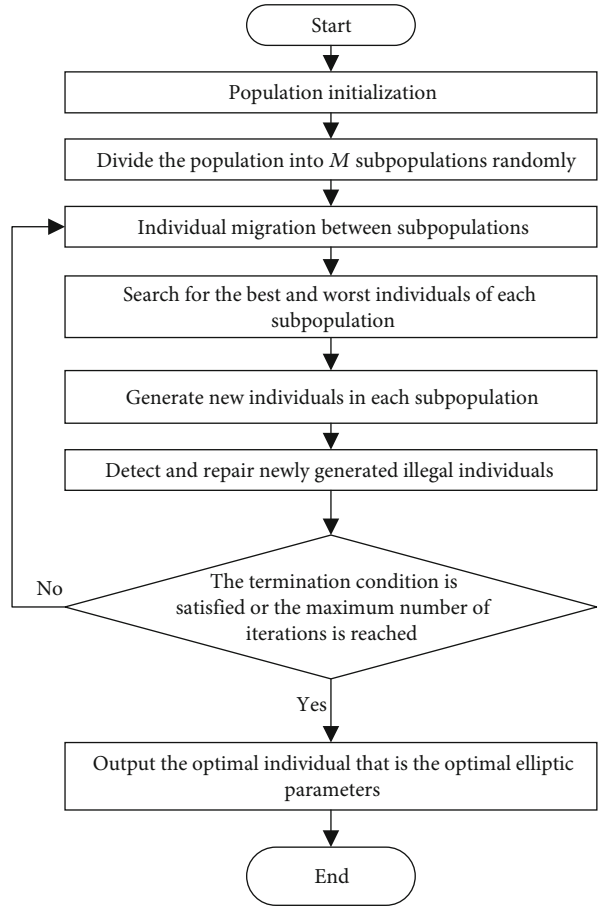

Figure 3: The flow chart of IHTJMC.

3.3. Implementation of IHTJMC. The implementation of IHTJMC is summarized as follows:

(1) Set the parameter initial values of the IHTJMC, such as the population size NP, the maximum number of iterations G, the number of the subpopulations M, and the stopping condition and T_f; then, generate the initial population through (5) and (6)

(2) Divide the whole population into M subpopulations according to Subpopulation Division

(3) Execute the migration between the different subpopulations according to Subpopulation Migration

(4) Calculate the best and worst individual of every subpopulation according to (10), and obtain the best and worst individual of the whole population through (11); then, generate new individual for each subpopulation by (7)

(5) Detect and treat illegal individuals according to (8) and update the population through (9)

Table 1: Test functions in experiment I.

Name	Expression formula	Dimension	Range
Sphere	$f_1(x) = \sum_{i=1}^{m} x_i^2$	5	[-100, 100]
Drop-wave	$f_2(x) = 1 + \cos\left(12\sqrt{x_1^2 + x_2^2}\right)/0.5\left(x_1^2 + x_2^2\right) + 2$	2	[-5.12, 5.12]
Girewank	$f_3(x) = 1/4000\sum_{i=1}^{m} x_i^2 + \prod_{i=1}^{m}\left(\cos x_i/\sqrt{i}\right)$	5	[-600, 600]
Rastrigin	$f_4(x) = \sum_{i=1}^{m} x_i^2 - 10\cos\left(2pi * x_i\right) + 10$	5	[-5.12, 5.12]
Rosenbrock	$f_5(x) = \sum_{i=1}^{m} 100\left(x_{i+1} - x_i^2\right)^2 + \left(x_i - 1\right)^2$	5	[-100, 100]
Schaffer	$f_6(x) = 0.5 + \left(\sin\sqrt{x_1^2 + x_2^2} - 0.5/\left[1 + 0.001\left(x_1^2 + x_2^2\right)\right]^2\right)$	2	[-100, 100]

(6) If the maximum number of iteration or stopping condition is reached, the optimal individual is output as the optimal solution; otherwise, return to step (3).

The flow chart of IHTJMC is shown in Figure 3 as follows.

4. Experiment and Result Analysis

In this section, three experiments are designed to test the superiority of the proposed method. The first experiment introduces six test functions to evaluate the performance of the proposed strategy based on the cooperation of multipopulation in the IHTJMC, which are widely used for the verification of the swarm intelligence optimization algorithms. The second is to test the performance of the IHTJMC through fitting a standard ellipse with some noise in simulation. The last one is to verify the performance of the IHTJMC for the diameter measurement with a red-hot gasket in a practical experiment.

4.1. Verification for Cooperation of Multiple Populations. In this experiment, six test functions including Sphere, Drop-wave, Girewank, Rastrigin, Rosenbrock, and Schaffer are introduced to test the effectiveness of the proposed strategy based on the cooperation of multiple populations in the IHTJMC. These functions are always utilized to verify the performance of the swarm intelligence optimization algorithms [31, 32]. They are shown in Table 1. At the same time, the unimproved Jaya which uses only one population is introduced into the comparison and the root mean square error (RMSE) is concerned as a performance index, and this experiment is implemented 30 times repeatedly and independently. The RMSE is calculated as follows:

$$\mathrm{RMSE} = \sqrt{\frac{1}{L}\frac{1}{K}\sum_{i=1}^{L}\sum_{j=1}^{K}\left(\widehat{x}_{i,j} - x_j\right)^2}, \tag{12}$$

where L is the number of independent experiments, $\widehat{x}_{i,j}$ is the $i_{\text{-th}}$ estimation of the $j_{\text{-th}}$ component, and x_j is the true value of the $j_{\text{-th}}$ component.

Table 2: RMSE of two methods in experiment I.

Function	Unimproved Jaya	Proposed
Sphere	2.3494e-19	7.8021e-20
Drop-wave	0.0019	0.0014
Girewank	6.8455	6.4910
Rastrigin	0.4698	0.3138
Rosenbrock	0.5389	0.1056
Schaffer	0.4058	0.0200

Table 2 shows the RMSE of the Jaya with only one population and the proposed strategy in 30 independent experiments, respectively. From Table 2, we can see that the RMSE of the Jaya with the proposed strategy for the six test functions is far superior to the unimproved Jaya. Compared with unimproved Jaya, the accuracy of the method with the proposed strategy is higher. This is because the cooperation of multipopulation can improve the diversity of the whole population, which possesses the strong ability of the information interaction between different subpopulations and the great evolutionary ability guided by multiple best and worst solutions.

Except for RMSE, the convergence curves of the methods are used to evaluate their convergence rates. The convergence curves of the Jaya with only one population and the proposed strategy for the six test functions are shown in Figures 4–9, respectively. These figures show that the Jaya with the proposed strategy has a higher convergence rate than the unimproved one. Especially in Figures 4–6, we can see that the unimproved Jaya traps into the local optimization and cannot jump out all the time. And the convergence curve of the Jaya with the proposed strategy is much better, because the global search capacity is enhanced due to the introduction of the cooperation of multiple populations. As a result, the search accuracy and convergence rate of the Jaya are significantly improved when the proposed strategy are added.

4.2. Ellipse Fitting Experiment. This experiment is used to verify the superiority of IHTJMC in the ellipse fitting. 100 data points are selected from an ellipse with Gaussian noise,

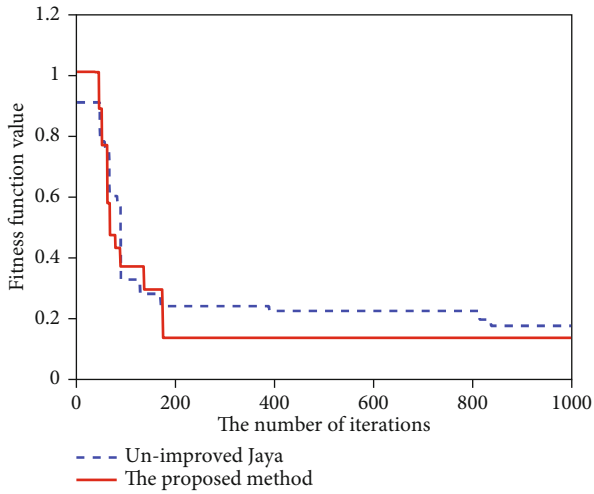

Figure 4: Convergence curves of Sphere with two methods.

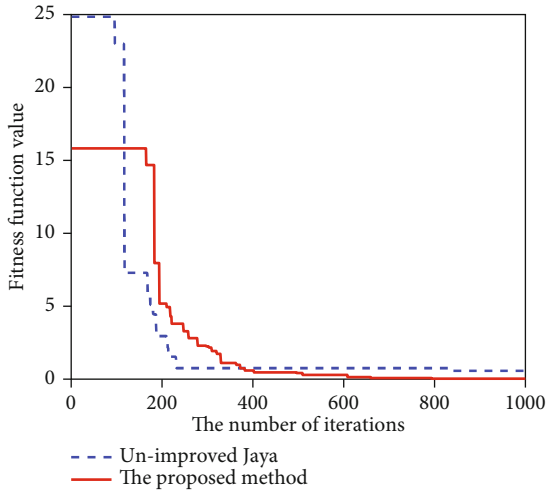

Figure 5: Convergence curves of Drop-wave with two methods.

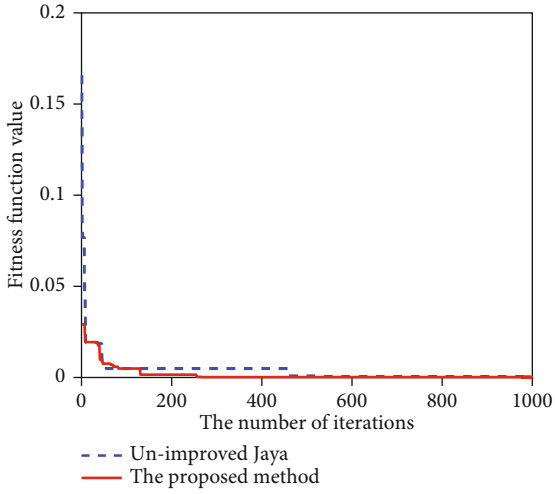

Figure 6: Convergence curves of Girewank with two methods.

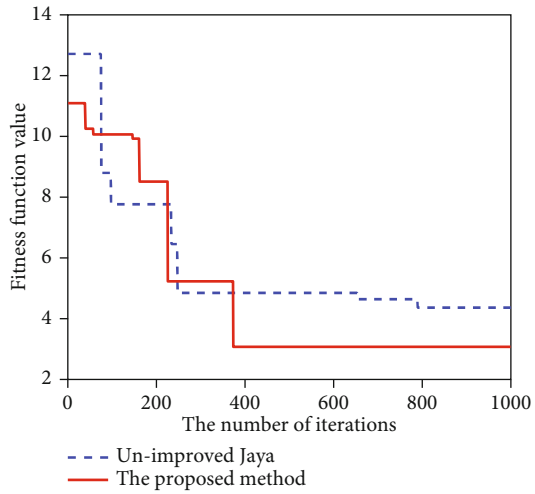

Figure 7: Convergence curves of Rastrigin with two methods.

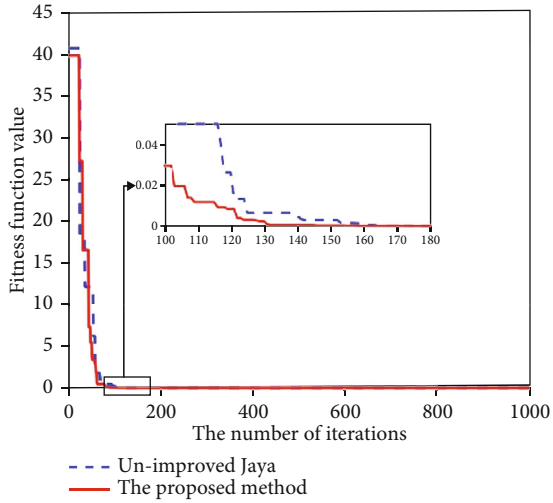

Figure 8: Convergence curves of Rosenbrock with two methods.

in which the parameters are set as $a = 7, b = 6, x_c = 9, y_c = 13$. The Gaussian noise variance is 0.01. These data points are shown in Figure 10. In order to test the superiority of IHTJMC better, a few existing methods including the IHTJ, direct least square (DLS), RHT, and RANSAC methods are introduced into the comparative evaluation. And RMSE is also considered as a performance index.

The parameter settings of these methods are as follows: the maximum number of iterations G is 1000, the number of the individuals NP is 90, T_f is 0.06, the termination condition is $Y_{gbest} > 94$, the number of subpopulations M is 3, the search scope is $[7 \pm 2, 6 \pm 2, 9 \pm 2, 13 \pm 2]$ (they are set double as large as those in [28]), and the experiment is also implemented 30 times repeatedly and independently.

Figure 11 provides the fitting results of these methods. We can see from this figure that the precision of the IHTJMC is better than those of other methods. Figure 12 presents the iteration curves of the fitness function with the IHTJ and IHTJMC, respectively. As shown in

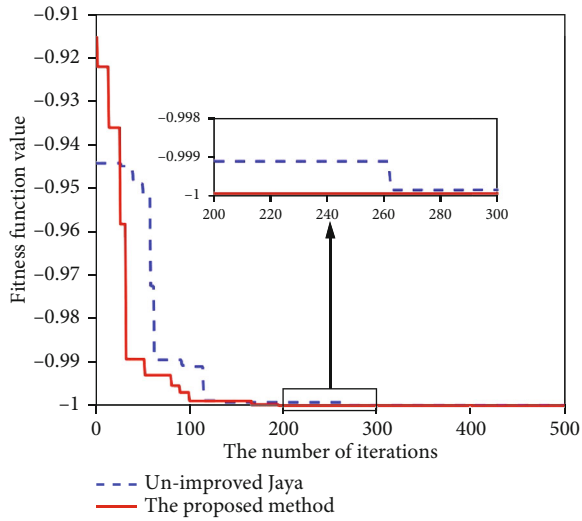

Figure 9: Convergence curves of Schaffer with two methods.

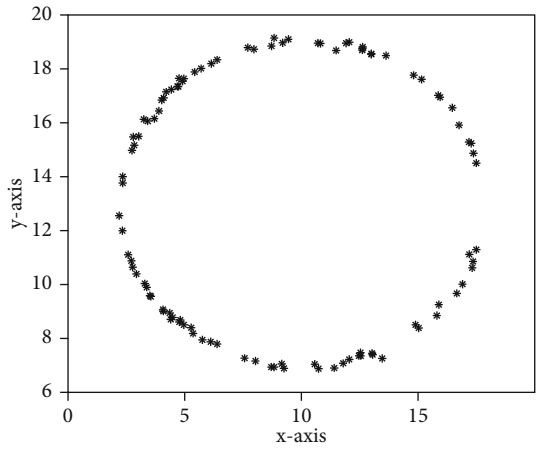

Figure 10: Ellipse data points containing Gaussian noise.

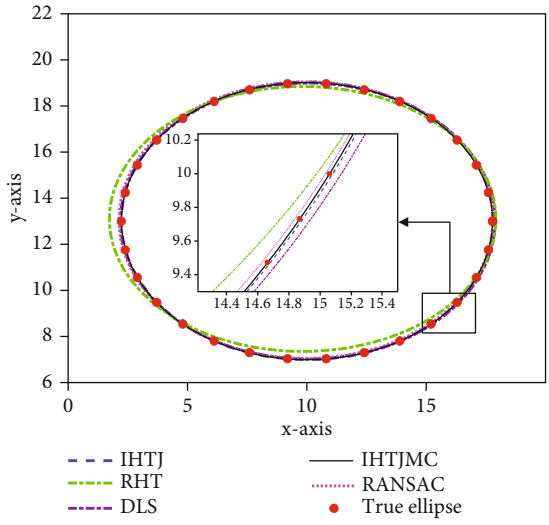

Figure 11: Comparative results of ellipse fitting in experiment II.

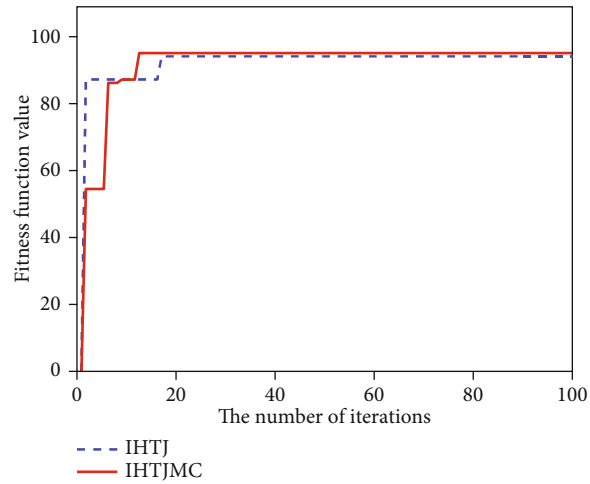

Figure 12: Iteration curves of fitness function with the IHTJ and IHTJMC in experiment II.

Table 3: RMSE of five methods in experiment II.

Method	a	b	x_c	y_c
IHTJMC	0.0115	0.0152	0.0081	0.0070
IHTJ	0.1248	0.0450	0.0704	0.0332
RHT	1.0612	0.7471	0.9324	0.6957
DLS	0.0621	0.0111	0.032	0.0078
RANSAC	0.2666	0.1154	0.2273	0.1556

Figure 12, the IHTJ converges at the $18_{\text{-th}}$ time, but the IHTJMC converges at the $13_{\text{-th}}$ time, so the convergence rate of the IHTJMC is superior to that of IHTJ. Moreover, the final value of fitness function of the IHTJ is less than that of the IHTJMC because the IHTJ has the problem of trapping into the local optimization, which is effectively suppressed in the IHTJMC through the introduction of the cooperation of multipopulation. Table 3 shows the RMSE of these methods in ellipse fitting, respectively. As shown in Table 3, the fitting accuracy of IHTJMC is much higher than those of other methods. As can be seen from these experimental results, the IHTJMC has better fitting accuracy than other methods. Compared with the IHTJ method, the IHTJMC has improved the fitting accuracy and convergence rate greatly when the search scope is doubled. This is because the cooperation strategy of multiple population strengthens the information exchange between the different subpopulations and can suppress the problem of the trapping local optimization effectively. As a result, it is very helpful to measure the workpiece's diameter accurately when the prior knowledge is inaccurate.

4.3. Diameter Measurement for Red-Hot Workpiece. To verify the IHTJMC for practical problems, it is used to measure the diameter of a gasket under high-temperature conditions. In this experiment, a CCD camera is used to capture image, and the edge point set which is used for ellipse fitting is obtained by image segmentation and edge extraction. Figure 13 is the image of the gasket under high temperature

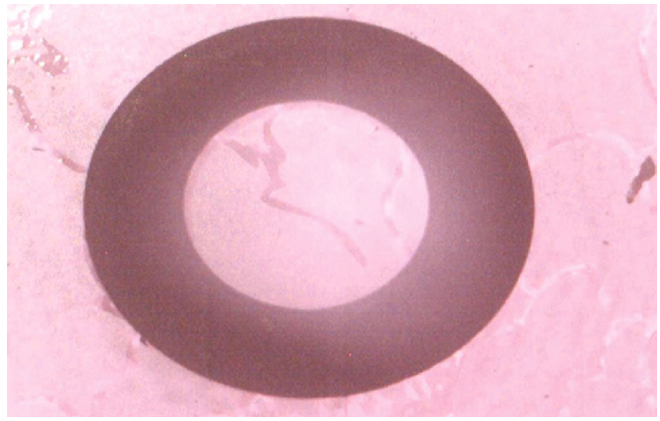

Figure 13: Image of red-hot gasket under high temperature.

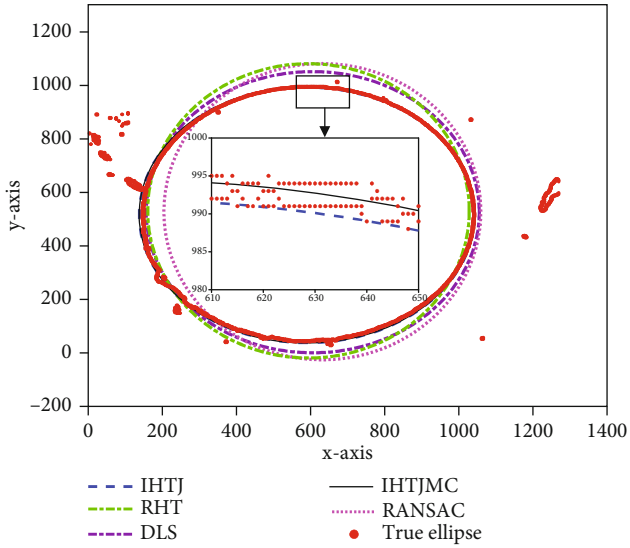

Figure 14: Ellipse fitting result of different methods in experiment III.

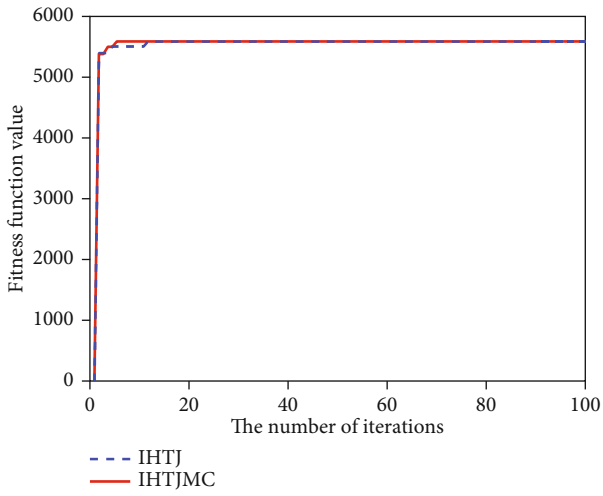

Figure 15: Iteration curves of fitness function with IHTJ and IHTJMC in experiment III.

Table 4: RMSE of diameter measurements with five methods in experiment III.

Method	RMSE
IHTJMC	0.0690
IHTJ	0.0959
RHT	4.3201
DLS	1.1412
RANSAC	1.9916

after the adjustment of CCD camera is finished. Because there is a shooting angle that is shown in Figure 1, the image of the gasket actually includes two ellipses: an inner ellipse and an outer ellipse. In this experiment, the diameter of the inner ellipse is used to calibrate, and the diameter of the outer ellipse is used to verify.

The parameters are set as follows: maximum number G of iterations is 1000, the number of the individuals NP is 90, the termination condition is $Y_{\text{gbest}} > 5600$, the number of subpopulations M is 3, the search scope is set twice as big as that in [28], and the experiment is run 30 times independently, too.

The results of ellipse fitting are shown in Figure 14. We can see from this figure that the result of the IHTJMC is closer to the true value compared with other methods, and the accuracy of the IHTJMC is highest. Figure 15 presents the iteration curves of fitness function in the IHTJ and IHTJMC, respectively. As shown in the figure, the IHTJ converges at the $12_{\text{-th}}$ time, and the IHTJMC converges at the $5_{\text{-th}}$ time. This proves that the convergence rate of the IHTJMC is superior to that of the IHTJ. Table 4 shows the comparison of RMSE of these methods. From the table, we can see that the accuracy of the IHTJMC for diameter measurement is much higher than those of other methods.

As can be seen from these experimental results, the measuring accuracy and converge rate are greatly raised after the improvement for the IHTJ with the cooperation strategy of multiple populations. It not only inherits the strengths of superior robustness and accuracy in HT but also overcomes the weakness of trapping into local optimization in the IHTJ and improves the accuracy and robustness of the IHTJ.

Therefore, the IHTJMC provides a more effective method for the diameter measurement in many complex industrial applications, especially the prior knowledge is inaccurate.

5. Conclusion

In this paper, IHTJMC is developed to address the disadvantage of the IHTJ in diameter measurement of a red-hot workpiece. In this method, a collaborative structure of multipopulation is proposed, and the migration strategy is designed to finish the cooperation between different subpopulations. The problem of trapping into local optimization is restrained and the global search ability is improved greatly. Three experiments are designed to test the effectiveness of the IHTJMC. Compared with the existing methods, the IHTJMC has better accuracy and robustness. It preserves the advantages of the IHTJ including high accuracy and strong robustness and improves the global search capacity of the IHTJ. It is beneficial to solve the problem of diameter measurement when the priori knowledge is not accurate. In future, how to restrain the effect of the error and the aberration during the measurement is an important subject in this field. At the same time, the better migration strategy will be further researched in the IHTJMC and the superior experimental scheme will be designed in the future.

Data Availability

In experiment I, six test functions including Sphere, Dropwave, Girewank, Rastrigin, Rosenbrock, and Schaffer are used to test the effectiveness of the proposed strategy based on the cooperation of multiple populations in the IHTJMC. These functions are always used to verify the performance of the swarm intelligence optimization algorithms. They are shown in Table 1 of the manuscript. In experiment II, 100 data points are selected from an ellipse with Gaussian noise, in which the parameters are set in the manuscript. The Gaussian noise variance is 0.01. These data points are shown in Figure 9 of the manuscript. The image of the last experiment can be obtained through sending an e-mail to the corresponding author.

Conflicts of Interest

The authors declare that there is no conflict of interest regarding the publication of this paper.

Acknowledgments

This work was supported by the National Natural Science Foundation (NNSF) of China [grant numbers 62003261, 61702410, 62073258, and 61871318] and Natural Science Basic Research Plan in Shaanxi Province of China [grant numbers 2020JQ-645 and 2020JQ-650].

References

[1] X. Pan, Z. Liu, and G. Zhang, "On-site reliable wheel size measurement based on multisensor data fusion," *IEEE Transactions on Instrumentation and Measurement*, vol. 68, no. 11, pp. 4575–4589, 2019.

[2] Y.-C. Zhang, C. Luo, X.-B. Fu, and Y. M. Chen, "Automatic measurement method for the size of large forgings based on scattering on rough surface," *IET Science, Measurement & Technology*, vol. 11, no. 1, pp. 118–124, 2017.

[3] S. Zhu, R. Huang, J. R. Avila et al., "Simultaneous measurements of wire diameter and conductivity using a combined inductive and capacitive sensor," *IEEE Sensors Journal*, vol. 20, no. 19, pp. 11617–11624, 2020.

[4] S. Babashakoori and M. Ezoji, "Average fiber diameter measurement in scanning electron microscopy images based on Gabor filtering and Hough transform," *Measurement*, vol. 141, pp. 364–370, 2019.

[5] M. Torabi, S. M. Mousavi, and D. Younesian, "A high accuracy imaging and measurement system for wheel diameter inspection of railroad vehicles," *IEEE Transactions on Industrial Electronics*, vol. 65, no. 10, pp. 8239–8249, 2018.

[6] X. Zhang, D. Liu, X. Wang, and X. Zhang, "Advanced ellipse fitting algorithm based on ADMM and hybrid BFGS method," *IEEE Transactions on Instrumentation and Measurement*, vol. 70, article 3515111, 2021.

[7] Y. Kang, J. Gong, Y. Xu et al., "Ultrahigh-precision diameter control of nanofiber using direct mode cutoff feedback," *IEEE Photonics Technology Letters*, vol. 32, no. 5, pp. 219–222, 2020.

[8] J. Jamaludin and R. A. Rahim, "Online optical tomography system for detecting and measuring the diameters of solid and transparent objects," *IEEE Sensors Journal*, vol. 16, no. 16, pp. 6175–6183, 2016.

[9] D. Liu and J. Liang, "A Bayesian approach to diameter estimation in the diameter control system of silicon single crystal growth," *IEEE Transactions on Instrumentation and Measurement*, vol. 60, no. 4, pp. 1307–1315, 2011.

[10] J. Liang, P. Li, D. Zhou et al., "Robust ellipse fitting via alternating direction method of multipliers," *Signal Processing*, vol. 164, pp. 30–40, 2019.

[11] M. Kesäniemi and K. Virtanen, "Direct least square fitting of hyperellipsoids," *IEEE Transactions on Pattern Analysis and Machine Intelligence*, vol. 40, no. 1, pp. 63–76, 2018.

[12] J. Liang, Y. Wang, and X. Zeng, "Robust ellipse fitting via half-quadratic and semidefinite relaxation optimization," *IEEE Transactions on Image Processing*, vol. 24, no. 11, pp. 4276–4286, 2015.

[13] P. C. Niedfeldt and R. W. Beard, "Convergence and complexity analysis of recursive-RANSAC: a new multiple target tracking algorithm," *IEEE Transactions on Automatic Control*, vol. 61, no. 2, pp. 456–461, 2016.

[14] T. Thomas, A. George, and K. I. Devi, "Effective iris recognition system," *Procedia Technology*, vol. 25, pp. 464–472, 2016.

[15] M. Kumar and N. B. Puhan, "RANSAC lens boundary feature based kernel SVM for transparent contact lens detection," *IET Biometrics*, vol. 8, no. 3, pp. 177–184, 2019.

[16] S. Huang, W. Jin, M. Ye et al., "A vision based method for automated measurement of circular fiber cross-sections," *Measurement*, vol. 162, article 107913, 2020.

[17] Y. Liu, J. Liu, and Y. Ke, "A detection and recognition system of pointer meters in substations based on computer vision," *Measurement*, vol. 152, article 107333, 2020.

[18] C. Lu, S. Xia, M. Shao, and Y. Fu, "Arc-support line segments revisited: an efficient high-quality ellipse detection," *IEEE Transactions on Image Processing*, vol. 29, pp. 768–781, 2020.

[19] R. O. Duda and P. E. Hart, "Use of the Hough transformation to detect lines and curves in pictures," *Communications of the ACM*, vol. 15, no. 1, pp. 11–15, 1972.

[20] N. Kiryati, Y. Eldar, and A. M. Bruckstein, "A probabilistic Hough transform," *Pattern Recognition*, vol. 24, no. 4, pp. 303–316, 1991.

[21] H. Yuen, J. Illingworth, and J. Kittler, "Detecting partially occluded ellipses using the Hough transform," *Image and Vision Computing*, vol. 7, no. 1, pp. 31–37, 1989.

[22] L. Xu, E. Oja, and P. Kultanen, "A new curve detection method: randomized Hough transform (RHT)," *Pattern Recognition Letters*, vol. 11, no. 5, pp. 331–338, 1990.

[23] V. Kumar, A. Asati, and A. Gupta, "Memory-efficient architecture of circle hough transform and its FPGA implementation for iris localisation," *IET Image Processing*, vol. 12, no. 10, pp. 1753–1761, 2018.

[24] L. Li, G. Wang, X. Zhang, and H. Yu, "Adaptive real-time recursive radial distance-time plane Hough transform track-before-detect algorithm for hypersonic target," *IET Radar, Sonar & Navigation*, vol. 14, no. 1, pp. 138–146, 2020.

[25] M. Liu, Z. Liu, W. Lu, Y. Chen, X. Gao, and N. Zhao, "Distributed few-shot learning for intelligent recognition of communication jamming," *IEEE Journal of Selected Topics in Signal Processing*, p. 1, 2021.

[26] M. Liu, J. Wang, N. Zhao, Y. Chen, H. Song, and R. Yu, "Radio frequency fingerprint collaborative intelligent identification using incremental learning," *IEEE Transactions on Network Science and Engineering*, 2021.

[27] M. Liu, C. Liu, M. Li, Y. Chen, S. Zheng, and N. Zhao, "Intelligent passive detection of aerial target in space-air-ground integrated networks," *China Communications*, vol. 19, no. 1, pp. 52–63, 2022.

[28] X. Zhang, R. Mu, K. Chen, Y. Yang, and Y. Chen, "Intelligent Hough transform with Jaya to detect the diameter of red-hot circular workpiece," *IEEE Sensors Journal*, vol. 21, no. 1, pp. 560–567, 2021.

[29] R. Rao, "Jaya: a simple and new optimization algorithm for solving constrained and unconstrained optimization problems," *International Journal of Industrial Engineering Computations*, vol. 7, no. 1, pp. 19–34, 2016.

[30] K. Gao, F. Yang, M. Zhou, Q. Pan, and P. N. Suganthan, "Flexible job-shop rescheduling for new job insertion by using discrete Jaya algorithm," *IEEE Transactions on Cybernetics*, vol. 49, no. 5, pp. 1944–1955, 2019.

[31] S. Zhang, J. Xu, L. H. Lee, E. P. Chew, W. P. Wong, and C. H. Chen, "Optimal computing budget allocation for particle swarm optimization in stochastic optimization," *IEEE Transactions on Evolutionary Computation*, vol. 21, no. 2, pp. 206–219, 2017.

[32] J. Tian, Y. Tan, J. Zeng, C. Sun, and Y. Jin, "Multiobjective infill criterion driven Gaussian process-assisted particle swarm optimization of high-dimensional expensive problems," *IEEE Transactions on Evolutionary Computation*, vol. 23, no. 3, pp. 459–472, 2019.